Science in China Series C: Life Sciences

www.scichina.com
life.scichina.com
www.springerlink.com

Expression profiling analysis for genes related to meat quality and carcass traits during postnatal development of backfat in two pig breeds

LI MingZhou[1*], ZHU Li[1*], LI XueWei[1†], SHUAI SuRong[1], TENG XiaoKun[2], XIAO HuaSheng[2], LI Qiang[1], CHEN Lei[1], GUO YuJiao[1] & WANG JinYong[3]

[1] College of Animal Science and Technology, Sichuan Agricultural University, Ya'an 625014, China;
[2] National Engineering Center for Biochip at Shanghai, Shanghai 201203, China;
[3] Chongqing Animal Husbandry Institute, Rongchang 402460, China

The competitive equilibrium of fatty acid biosynthesis and oxidation *in vivo* determines porcine subcutaneous fat thickness (SFT) and intramuscular fat (IMF) content. Obese and lean-type pig breeds show obvious differences in adipose deposition; however, the molecular mechanism underlying this phenotypic variation remains unclear. We used pathway-focused oligo microarray studies to examine the expression changes of 140 genes associated with meat quality and carcass traits in backfat at five growth stages (1—5 months) of Landrace (a leaner, Western breed) and Taihu pigs (a fatty, indigenous, Chinese breed). Variance analysis (ANOVA) revealed that differences in the expression of 25 genes in Landrace pigs were significant (FDR adjusted permutation, $P<0.05$) among 5 growth stages. Gene class test (GCT) indicated that a gene-group was very significant between 2 pig breeds across 5 growth stages ($P_{ErmineJ}<0.01$), which consisted of 23 genes encoding enzymes and regulatory proteins associated with lipid and steroid metabolism. These findings suggest that the distinct differences in fat deposition ability between Landrace and Taihu pigs may closely correlate with the expression changes of these genes. Clustering analysis revealed a very high level of significance (FDR adjusted, $P<0.01$) for 2 gene expression patterns in Landrace pigs and a high level of significance (FDR adjusted, $P<0.05$) for 2 gene expression patterns in Taihu pigs. Also, expression patterns of genes were more diversified in Taihu pigs than those in Landrace pigs, which suggests that the regulatory mechanism of micro-effect polygenes in adipocytes may be more complex in Taihu pigs than in Landrace pigs. Based on a dynamic Bayesian network (DBN) model, gene regulatory networks (GRNs) were reconstructed from time-series data for each pig breed. These two GRNs initially revealed the distinct differences in physiological and biochemical aspects of adipose metabolism between the two pig breeds; from these results, some potential key genes could be identified. Quantitative, real-time RT-PCR (QRT-PCR) was used to verify the microarray data for five modulated genes, and a good correlation between the two measures of expression was observed for both 2 pig breeds at different growth stages ($R=0.874\pm0.071$). These results highlight some possible candidate genes for porcine fat characteristics and provide some data on which to base further study of the molecular basis of adipose metabolism.

pig, adipose, microarray, differential gene expression, clustering analysis, gene regulatory network (GRN)

Because of consumers' demands, the emphasis of modern day porcine breeding programs and selection criteria is gradually shifting towards a higher meat quality, instead of the more classical focus of just selecting for a lean carcass and high growth rate[1]. A strongly genetically determined factor influencing carcass composition is the backfat thickness (BFT). Intramuscular fat (IMF)

Received January 30, 2007; accepted April 5, 2008
doi: 10.1007/s11427-008-0090-0
†Corresponding author (email: lixuewei9125@126.com)
*Contributed equally to this wrok
Supported by the Program for Changjiang Scholars and Innovative Research Team in University of Chinese Ministry of Education (Grant No. IRT0555-6), Specialized Research Fund for the Doctoral Program of Higher Education of China (Grant No. 20060626003), National Sci &Tech Support Program (Grant No. 2007BAD51B03), Project of Provincial Eleventh 5 Years' Animal Breeding of Sichuan Province (Grant No. 2006YZGG-15), and Specialized Research Fund of Chinese Ministry of Agriculture (Grant No. NYHYZX07-034)

content is a major determinant of pork quality. In particular, tenderness, flavor, juiciness, water-holding capacity, acceptability of fresh meat, and eating quality are all influenced by the amount of IMF[2]. However, genetic correlations (r_G) of IMF content with other carcass traits are unfavorable and moderate, such as the r_G of IMF content with *longissimus dorsi* muscle area (LMA) and BFT, which were –0.26 and 0.28, respectively[3]. Unfortunately, the selection of leaner pigs was often accompanied by a decrease in IMF content and BFT, resulting in a decrease of meat quality. At present, many pig breeding companies attempt to generate, through DNA marker assistant selection (MAS), pigs that have both improved meat quality and lean carcasses[2].

The metabolism of adipose is a complex physiological process involving co-expressional and co-restricted multi-genes. The competition between rates of fatty acid biosynthesis and oxidation *in vivo* determines fat deposition and distribution. In recent years, adipose tissue is well recognized as a highly active endocrine organ, more than just a passive repository for excess energy. A radical change in perspective followed the discovery of a large number of proteins secreted from white adipocyte, such as proinflammatory cytokines, chemokines, growth factors and complement proteins collectively called "adipokines" or "adipose tissue hormones"[4]. The effects of adipokines may be either autocrine or paracrine, meaning that they might act in adipose tissue itself or in more distant target tissues. At present, little is known about the biological functions of adipokines, and in particular, the intracellular signal transduction mechanism remains only partially understood. In a post-genomic era, functional genomics, including parallel analysis of gene expression (the transcriptome and proteome), provides new opportunities to identify pathways and interacting genes and how these influence porcine fat deposition.

Breed differences in meat quality and carcass traits are large. Western pig breeds have been intensively selected over the past two decades for rapid, large and efficient descent of fat, which is believed to have led to deterioration in meat quality. Landrace, a typical lean-type western breed, is now widely used for commercial production throughout the world. While indigenous Chinese pig breeds have lower growth rates and a higher fat content than conventional western pig breeds, they have proved superior in terms of perceived meat quality and carcass composition. The Taihu variety is a typical indigenous Chinese breed of pig[5].

Here, we describe a pathway-focused analysis of gene expression changes in backfat in Landrace and Taihu pigs at 1—5 months. Our results could be beneficial to researchers attempting to identify the candidate genes that contribute to variation in porcine meat quality and carcass traits.

1 Materials and methods

1.1 Animals and tissue preparation

Landrace and Taihu pigs (10 sows and 10 boars for each breed) were used in this study. Two male and two female piglets were randomly assigned to each stage for each breed with ad libitum access to feed under same normal conditions. The piglets were weaned simultaneously at 28±1 d of age. The animals were reared in compliance with national regulations for the humane care and use of animals in research. The pigs were sacrificed at a commercial slaughterhouse at 1—5 months of age. The backfat tissue near the last 3rd or 4th rib was rapidly and manually dissected from each cleaved pig. These samples (thickness 0.3 — 0.4 cm) were immediately submerged in RNA*later* (Qiagen, Germany) for RNA preservation, after which they were crushed to powder with liquid nitrogen, subdivided per 160—200 mg and stored at –70℃ until further use.

1.2 Adipose measurements

After being sacrificed, all adiposes were fixed in 10% neutral buffered formalin solution, embedded in paraffin using TP1020 semi-enclosed tissue processor (Leica, Germany), sliced at a thickness of 6 μm using RM2135 rotary microtome (Leica, Germany) and stained with hematoxylin and eosin (H&E). The mean diameter of an adipocyte cell was calculated by geometric average of the max- and min-diameter, and 100 cells were measured for each sample in randomly selected fields using a TE2000 fluorescence microscope (Nikon, Japan) and Image Pro-Plus 6.0 software (Media-Cybernetics, USA). The mean adipocyte cell volume (V) was obtained according to the following formula:

$$V = \pi/6 \sum f_i D_i^3 / \sum f_i,$$

where D_i is the mean diameter; f_i denotes the cell numbers of mean diameter D_i. The IMF content was measured by heat extraction-oil weight method using Soxte-

cAvanti2055 extraction system (Foss, Denmark).

1.3 Construction of porcine pathway-focused microarray

One hundred and forty genes that were involved in biological processes of adipose metabolism and muscle growth were selected with the aid of gene annotations of Gene Ontology (GO) terms and hundreds of biomedical literatures using Onto-Design[6] and GoPubMed[7] tools. The set of 140 oligonucleotides (Pig Genome Oligo Microarray Database, http://omad.operon.com/pig/query.php) represents porcine cDNAs and ESTs and was designed from TIGR TC cDNA sequences (SsGI release 12.0, http://compbio.dfci.harvard.edu/tgi/cgi-bin/tgi/gimain.pl?gudb=pig). In addition, there were six positive control genes and six negative controls including three *Arabidopsis* genes and three randomized sequences known to have minimal cross-hybridization with mammalian transcripts. All pig-specific ~70 mer oligonucleotides were designed within 1000 bp of an annotated 3′ end, with the cross-oligonucleotide percentage identity <70%. No oligonucleotide has 20 contiguous bases in common with any other oligonucleotide. No oligonucleotide has repeats >8 bases or a potential hairpin stem >9 bp.

The synthesized oligonucleotides were spotted at the National Engineering Eenter for Biochip at Shanghai, China. Each oligonucleotide was spotted four times and each control gene was spotted eight times on GAPS II slides (Corning, USA) using OmniGrid100 microarrayer (Gene-Machine, USA). Oligonucleotides were ultraviolet (UV) cross-linked to the slides after spotting according to the manufacturer's protocol for all slides. All information about this pathway-focused oligo microarray has been submitted to the NCBI Gene Expression Omnibus (GEO) database under the accession number GPL5171.

1.4 Experimental design

Temporal gene expression changes within breeds were analyzed with microarrays using a direct loop design that included two independent loops, for a total of five arrays per loop. Breed changes in gene expression at the same month were analyzed with microarrays using a matched-pair design that included five arrays[8]. Data from 30 measurements from 15 arrays were collected (Figure 1). It should be noted that the three replicate measurements for each sample and the four replicate printings per slide represent technical variation. Biological variation was sampled by extracting RNA from four separate samples and pooling them before all of the hybridizations.

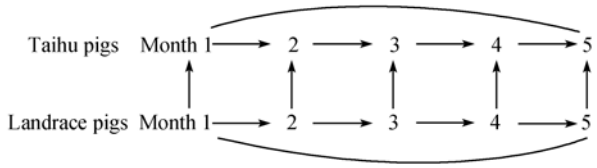

Figure 1 A modified loop microarray experimental designs for temporal and breed studies. The arrow from tail to head indicates Cy5 to Cy3 dye.

1.5 RNA and target preparation for hybridization

Total RNA was prepared from the frozen backfat using RNeasy Lipid Tissue Min kit (Qiagen, Germany) according to the manufacturer's protocol for all samples. The purified RNA was examined by 1% agarose gel electrophoresis and quantified using an Agilent2100 bioanalyzer (Agilent, USA). Equal quantities of total RNA from four individuals (two sows and two boars at each stage for each breed) were pooled. Cy3- and Cy5-labeled cRNAs were prepared and hybridized to slides at 42℃ for 12－14 h using Low RNA Input Linear Amplification Plus-two Color kit (Agilent, USA) and Pronto Universal Hybridization kit (Corning, USA) according to the manufacturer's protocol. Finally, slides were dried by centrifugation at 2500 r/min for 2 min and stored in the lightproof container until ready to scan.

1.6 Image processing

The slides were scanned at 532 nm (for Cy3) and 635 nm (for Cy5) using the ScanArray4000 scanner (Perkin-Elmer, USA) under conditions to limit saturation to <1%. Scanned images were analyzed using ImaGene7.5 software (Bio-Discovery, USA). Defective microarray spots (signal-to-background ratio 2.5 or 40% spot area compared with average) were eliminated from the data set. These criteria assured that the signal level was sufficiently high above background to be reliably read and that the reading was not the result of non-uniform noise emanating from the spotted oligonucleotides.

1.7 Normalization of microarray data

Local background values and negative control values were subtracted from signal means respectively, and a small constant was added to all differences to allow for log transformation of the background-corrected signals.

Following log transformation, composite loess and print-tip loess normalization were applied to remove intensity-dependent dye bias from each slide using WebArray online platform (Sidney Kimmel Cancer Center, USA) (http://bioinformatics.skcc.org/webarray)[9,10]. Four replicate spots within-array were incorporated using pooled correlation method[11]. The resulting values were adjusted so that the median normalized signal for each gene would be constant across all slide and dye combinations. Here, each array provided with two following observations for each gene: log intensity ratios $M=\log_2 Cy3-\log_2 Cy5$ and mean log intensities $A=(\log_2 Cy3+\log_2 Cy5)/2M$. The normalized data were then back-transformed prior to further statistical analysis using the following formulas:

$$\log_2 Cy3=A+M/2 \text{ and } \log_2 Cy5=A-M/2.$$

Genes were filtered with more than 70% missing (across arrays), then missing values were imputed using 5-nearest neighbour method[12]. All raw microarray data have been deposited in the NCBI GEO database with the accession number GSE7856.

1.8 Differential gene expression analysis

An extended variance analysis (ANOVA) modeling approach was used to analyze the microarray data using the J/maanova package (The Jackson Laboratory, USA)[13]. To analyze the breed effect across five time points and time effect across two pig breeds with a simultaneous consideration of all blocking factors used in the experimental design, a gene-specific model was applied:

$$\log_2(Y_{ijklmn}) = \mu + A_i + D_j + B_k + T_l + S_m + \varepsilon_{ijklmn},$$

where Y_{ijklmn} denotes the fluorescent intensity signal of the nth gene (n=1, ···, 95), ith array (i=1, ···, 15), jth dye (j=1, 2), kth breed (k=1, 2), lth month (l=1, ···, 5) and sth RNA pool (s=1, ···, 10); μ is an overall mean value; A_i is the fixed effect of array i; D_j is the fixed effect of dye j; B_k is the fixed effect of breed k; T_l is the fixed effect of month l; S_m is the random effect of RNA pool m and ε_{ijklmn} is a stochastic error (assumed to be normally distributed with mean 0 and variance σ^2). Identification of time effects for each pig breed was also performed using the gene-specific model:

$$\log_2(Y_{ijklm}) = \mu + A_i + D_j + T_k + S_l + \varepsilon_{ijklm},$$

where Y_{ijklm} denotes the fluorescent intensity signal of the mth gene (n=1, ···, 95), ith array (i=1, ···, 15), jth dye (j=1, 2), kth month (k=1, ···, 5) and lth RNA pool (l=1, ···, 10); μ is an overall mean value; A_i is the fixed effect of array i; D_j is the fixed effect of dye j; T_k is the fixed effect of month k; S_l is the random effect of RNA pool l and ε_{ijklm} is a stochastic error (assumed to be normally distributed with mean 0 and variance σ^2). Variance components of mixed linear model (MME) were estimated using restricted maximum likelihood (REML) method and false discover rate (FDR) was controlled using Step Down method. The FDR adjusted permutation P values were generated after iterating 10 000 times, which were obtained from empirical Bayes test based on shrinkage estimates of variance components[14].

1.9 Gene class test (GCT)

GCT analysis was performed using ErmineJ software (Columbia University, USA)[15]. Genes with similar biological functions were clustered into a same gene-group based on existing GO annotations and relative literatures. The FDR adjusted permutation P values of above ANOVA were analyzed using gene score resampling (GSR) algorithm under 200 000 times iterations to determine which gene-group was significant below Benjamini-Hochberg FDR-corrected P value of 0.05 or 0.01.

1.10 Clustering analysis

Gene expression patterns during the investigated five growth stages were identified using Short Time-series Expression Miner (STEM) software (Carnegie Mellon University, USA)[16]. The $\log_2$-transformed fluorescent intensity signals were subjected to clustering. All data sets were filtered to contain only the 93 genes that exhibited a two-fold increase or decrease for at least one time point within pig breeds. The filtered data sets were divided into 9 predetermined temporal expression patterns with the two times of maximum unit change in model profiles between two discretionary time points. FDR-corrected P values from multiple hypothesis test (MHT) were obtained to determine the significance of each expression pattern.

1.11 Reconstruction of gene regulatory network (GRN)

GRNs were reconstructed from time-series data for each pig breed using GeneNetwork software (Yang-Ming University, Taiwan, China)[17]. Complex relationships among genes were inferred based on dynamic Bayesian network (DBN) model under the fixed discretized threshold (2× SD)[18].

1.12 Quantitative real-time RT-PCR (QRT-PCR)

QRT-PCR (SYBR Green I) analysis was performed on five differentially expressed genes, *IGF-II, IGFBP3, SCD, ME1* and *UCP3*, each normalized to *ACTB*, *TBP* and *TOP2B*[19]. Primers of 8 target sequences were designed using Primer-3 online platform (http://frodo.wi.mit.edu/) (Table 1). Pooled RNA of each stage and breed collected for the microarray analysis were also used for QRT-PCR analysis. Two-step reverse transcription PCR method was used to generate cDNA using SYBR PrimeScript RT-PCR kit (TaKaRa, Japan) according to the manufacturer's protocol. Real time fluorescent measuration was conducted on the iQ5 real-time PCR detection system (Bio-Rad, USA). A 10-fold dilution series of cDNA were included in each run to determine PCR efficiency by constructing a relatively standard curve. PCR efficiencies were consistently >92% and were used to convert the cycle threshold (Ct) values into raw data. All experiments contained a negative control and samples were analyzed in three independent runs. Normalized factors of internal control genes and relative quantities of objective genes were analyzed using GeNorm software (Primer-Design, UK)[20].

Table 1 Information on the primers used for QRT-PCR

Gene symbol	Primer sequence(5′→3′)	Amplicon length/bp	Annealing temperature (℃)	GenBank No.
ACTB	TCTGGCACCACACCTTCT	114	62	DQ178122
	TGATCTGGGTCATCTTCTCAC			
TBP	GATGGACGTTCGGTTTAGG	124	60	DQ178129
	AGCAGCACAGTACGAGCAA			
TOP2B	AACTGGATGATGCTAATGATGCT	137	60	AF222921
	TGGAAAAACTCCGTATCTGTCTC			
IGF-II	ACACCCTCCAGTTTGTCTGCG	108	61	X56094
	CAGCTACGGAAGCAGCACTCT			
IGFBP3	CCAGCGCTACAAGGTCGACTAC	73	61	AF085482
	TCTCGCGCTTGGACTCAGA			
SCD	AAGGAACTAGAAGGCTGCTC	211	61	AY487829
	TGTAGAGCAGCAGCCATCAC			
ME1	TGAAGAACCTAGAAGCCATT	242	60	X93016
	AAGAGTGACCGGATCAAAAG			
UCP3	ACGATGGATGCCTACAGGAC	200	61	DQ530368
	TCCGAAGGCAGAGACAAAGT			

ACTB (*β* actin), *TBP* (TATA box binding protein) and *TOP2B* (topoisomerase II *β*) are the internal control genes.

2 Results

2.1 Body weight and fat characteristics

Histological structures of adipocyte cells were clear after H&E staining, and the differences among cells could be identified by quantitative image analysis (Figure 2). Landrace pigs exhibited a higher body weight than Taihu pigs at all stages except at the 4-month. However, Taihu pigs had a higher adipocyte volume and IMF content than Landrace pigs from 1 to 5 months, and the gaps were more obvious after 3-month and especially at 5-month, when there were 2.25 and 2.05-fold differences for the above two indexes, respectively (Figure 3).

2.2 Significance tests for differential gene expression and gene-groups

The modified loop designs utilized in this study are discussed in "Materials and Methods" and outlined in Figure 1. This approach allows comparison among all conditions via the ANOVA model. Using FDR adjusted permutation *P* values, we found that there were 25 genes showing differential expression at $P<0.05$ among 5 growth stages in Landrace pigs (Table 2).

To reduce the interpretive challenge posed by the long list of differentially expressed genes and to obtain a global picture of the affected processes, we used GCT analysis based on twelve prearranged gene-groups. Us-

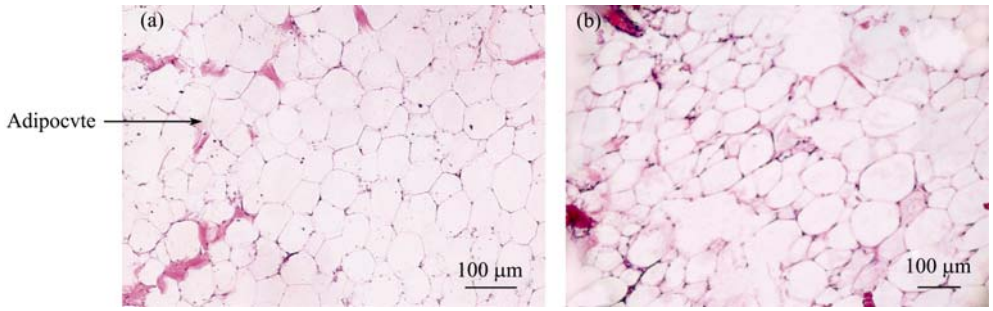

Figure 2 Representative pictures of the enlarged adipocytes from Landrace (a) and Taihu pigs (b) at 5-month.

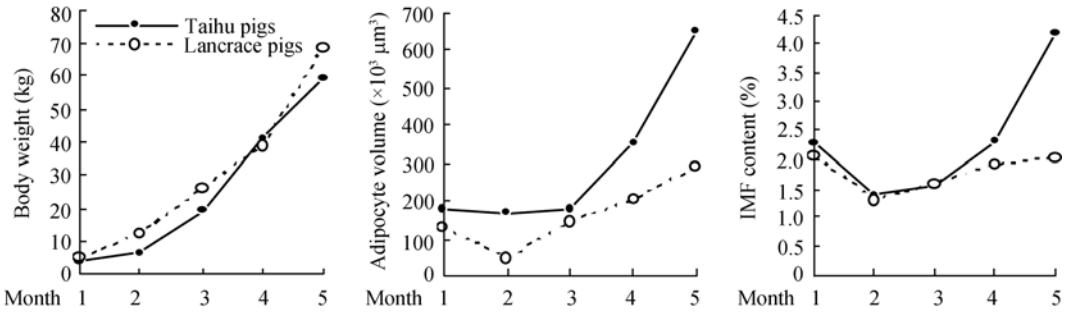

Figure 3 Developmental changes in body weight (a), adipocyte volume (b) and IMF content (c).

ing Benjamini-Hochberg FDR-corrected P values, we found that there were two very significant gene-groups ("enzymes and regulatory proteins related to lipid and steroid metabolism" and "myogenic determination factors", $P_{\text{ErminеJ}}<0.01$) between two pig breeds across five growth stages. In addition, one gene-group was very significant ("enzymes related to glucose metabolism", $P_{\text{ErminеJ}}<0.01$) in Taihu pigs across five growth stages (Table 2).

2.3 Clustering of time-series data (STEM)

The predominant temporal expression patterns were identified using a unique STEM algorithm (Figure 4). Two expression patterns for each pig breed were judged to be statistically significant between the number of genes expected ($n_{(E)}$) and the number of genes assigned (n) and potentially contained genes that were coordinately regulated. Expression patterns 1 ($n_{(E)}$=11.7, n=23) and 8 ($n_{(E)}$=10.9, n=35) for Landrace pigs showed differential gene numbers at $P<0.01$ and, expression patterns 7 ($n_{(E)}$=10, n=17) and 8 ($n_{(E)}$=11.1, n=19) for Taihu pigs had a $P<0.05$. Of these patterns, expression pattern 1 of Landrace pigs represented genes that were strongly down-regulated from 1 to 5 months; the trendline of the log of the expression change ratio over all stages fitted a straight line of 0, −1, −2, −3, and −4. Expression pattern 7 of Taihu pigs represented genes that were first up-regulated to a highest expression level at 3-month, then down-regulated to the original level; the trendline of the log of the expression change ratio over all stages fitted a curve of 0, 1, 2, 1, and 0. Expression pattern 8 of the two pig breeds represented genes that were strongly up-regulated from 1 to 5 months; the trendline of the log of the expression change ratio over all stages fitted a straight line of 0, 1, 2, 3, and 4.

2.4 GRN of time-series data (DBN model)

The complex relationships among genes associated with meat quality and carcass traits in porcine backfat were inferred using a DBN model. The reconstructed sub-network for Landrace pigs included 68 nodes that represented corresponding genes (Figure 5(a)). Of these, as a leading parent node, *OB* directly regulated *DCTN6*, *LIPE*, *TCAP*, *TGFB3* and *UCP2*. As a leading child node, *TCAP* was directly regulated by 38 genes. The reconstructed sub-network for Taihu pigs consisted of 76 nodes (Figure 5(b)). Of these, as a leading parent node, *ANGPTL4* directly regulated *LPL*, *MYOG*, *RYR1*, *TTN* and *UCP2*. As leading child nodes, *TTN* and *UCP2* were directly regulated by 45 and 48 genes, respectively

Table 2 Results of ANOVA, GCT and STEM clustering

ID	Gene name/ gene-group description	Gene symbol	P_1	P_2	P_3	P_4	Cluster ID
a	Enzymes and regulatory proteins related to lipid and steroid metabolism						
	$P_{\text{ErminеJ}}$ (n_a=23)		0.000	0.065	0.862	1.000	
1	Acetyl-CoA acyltransferase 1	*ACAA*	0.963	0.792	0.601	0.796	8|1
2	Acyl-CoA dehydrogenase, long chain	*ACADL*	0.904	0.465	0.080	0.656	8|6
3	Acyl-CoA dehydrogenase, C-4 to C-12 straight chain	*ACADM*	0.886	0.591	0.465	0.656	6|8
4	Acyl-CoA dehydrogenase, C-2 to C-3 short chain	*ACADS*	0.674	0.447	0.577	0.558	\
5	Angiopoietin-like 4	*ANGPTL4*	0.886	0.235	0.016	0.558	1|1
6	3-hydroxybutyrate dehydrogenase, type 2	*BDH2*	0.886	0.838	0.514	0.568	2|0
7	Carnitine palmitoyl transferase 1B	*CPT1B*	0.963	0.699	0.202	0.601	4|8
8	Crystallin λ1	*CRY*	0.886	0.493	0.202	0.558	0|1
9	Dodecenoyl-CoA δ isomerase	*DCI*	0.886	0.426	0.202	0.558	8|7
10	Diacylglycerol *O*-acyltransferase	*DGAT*	0.963	0.184	0.051	0.558	8|7
11	Dehydrogenase/reductase (SDR family) 3	*DHRS3*	0.963	0.689	0.031	0.984	8|6
12	Enoyl-CoA hydratase 1, peroxisoma 1	*ECH1*	0.886	0.184	0.202	0.558	8|7
13	Enoyl CoA hydratase, short chain, 1, mitochondrial	*ECHS1*	0.693	0.184	0.037	0.656	8|7
14	Hydroxyacyl-CoA dehydrogenase	*HAD*	0.886	0.484	0.080	0.601	8|0
15	Hydroxyacyl-CoA dehydrogenase/3-etoacyl-CoA thiolase/ enoyl-CoA hydratase, α subunit	*HADHA*	0.528	0.426	0.362	0.558	1|1
16	Hydroxysteroid (17β) dehydrogenase 4	*HSD17B4*	0.997	0.591	0.305	0.656	8|0
17	Long-chain 3-ketoacyl-CoA thiolase	*LCTHIO*	0.886	0.773	0.490	0.984	\
18	Hormone sensitive lipase	*LIPE*	0.886	0.817	0.164	0.604	0|1
19	Propionyl-CoA carboxylase, β polypeptide	*PCCB*	0.886	0.235	0.031	0.601	8|7
20	Phospholipase D2	*PLD2*	0.845	0.465	0.302	0.818	2|2
21	Aphosphatidic acid phosphatase type 2A	*PPAP2A*	0.886	0.649	0.219	0.868	2|1
22	Peroxiredoxin 6	*PRDX6*	0.886	0.184	0.052	0.568	8|8
23	Sterol-C4-methyl oxidase-like	*SC4MOL*	0.886	0.640	0.039	0.835	5|0
b	Enzymes and regulatory proteins related to proteolysis						
	$P_{\text{ErminеJ}}$ (n_b=7)		1.000	0.774	0.941	1.000	
24	Calpain 2, (m/II) large subunit	*CAPN2*	0.886	0.515	0.357	0.872	3|3
25	Calpain 3, (p94)	*CAPN3*	0.810	0.235	0.184	0.679	4|0
26	Calpain, small subunit 1	*CAPNS1*	0.886	0.532	0.325	0.558	0|1
27	Cystatin B (stefin B)	*CSTB*	0.909	0.426	0.232	0.656	0|0
28	Cathepsin D	*CTSD*	0.886	0.465	0.144	0.836	3|0
29	Cathepsin K	*CTSK*	0.958	0.786	0.043	0.568	8|4
30	Cathepsin L2	*CTSL2*	0.886	0.565	0.363	0.558	2|2
c	Enzymes related to glucose metabolism						
	$P_{\text{ErminеJ}}$ (n_c=5)		1.000	0.322	0.732	0.000	
31	Enolase 3β	*ENO3*	0.845	0.184	0.037	0.558	1|1
32	Glycerol-3-phosphate dehydrogenase 1	*GPD1*	0.886	0.235	0.064	0.380	7|8
33	Lactate dehydrogenase A	*LDHA*	0.963	0.484	0.047	0.558	1|5
34	Lactate dehydrogenase B	*LDHB*	0.958	0.785	0.202	0.601	8|0
35	UDP-glucose pyrophosphorylase 2	*UGP2*	0.963	0.465	0.297	0.679	5|8

(*To be continued on the next page*)

(*Continued*)

ID	Gene name/ gene-group description	Gene symbol	P_1	P_2	P_3	P_4	Cluster ID
d	Enzymes related to glucose biosynthesis						
	$P_{\text{ErminеJ}}$ (n_d=2)		1.000	0.969	0.900	1.000	
36	Glycogen synthase 1	*GYS1*	0.886	0.640	0.204	0.660	1|7
37	Phosphoglucomutase 1	*PGM1*	0.958	0.847	0.047	0.656	1|8
e	Enzymes related to fatty acid biosynthesis						
	$P_{\text{ErminеJ}}$ (n_e=11)		1.000	0.110	0.676	1.000	
38	Protein kinase, AMP activated, α2 catalytic subunit	*AMPKA2*	0.963	0.484	0.297	0.818	7|8
39	Dynactin 6	*DCTN6*	0.845	0.447	0.618	0.558	3|0
40	Isocitrate dehydrogenase 2 ($NADP^+$)	*IDH2*	0.974	0.465	0.026	0.558	1|2
41	Lipoprotein lipase	*LPL*	0.997	0.754	0.035	0.660	8|7
42	Malate dehydrogenase 1, NAD (soluble)	*MDH1*	0.886	0.235	0.208	0.380	8|7
43	Malate dehydrogenase 2, NAD(mitochondrial)	*MDH2*	0.886	0.658	0.216	0.852	0|8
44	Malic enzyme 1, $NADP(^+)$-dependent	*ME1*	0.886	0.235	0.026	0.568	8|7
45	NADH dehydrogenase 1, α/β subcomplex, 1, 8 kD	*NDUFAB1*	0.886	0.184	0.325	0.380	8|8
46	Phosphogluconate dehydrogenase	*PGD*	0.963	0.864	0.202	0.558	1|8
47	Stearoyl-CoA desaturase	*SCD*	0.886	0.184	0.033	0.558	8|8
48	Triosephosphate isomerase 1	*TPI1*	0.963	0.817	0.097	0.897	1|5
f	Binding proteins and transfer proteins related to fatty acid transport						
	$P_{\text{ErminеJ}}$ (n_f=8)		0.096	1.000	0.867	0.977	
49	Adipose differentiation related protein	*ADRP*	0.886	0.864	0.505	0.604	7|2
50	Apolipoprotein A-II	*APOA2*	0.886	0.447	0.498	0.558	7|8
51	Caveolin 1, caveolae protein, 22 kD	*CAV1*	0.886	0.754	0.204	0.843	8|0
52	Fatty acid binding protein 3, muscle and heart	*FABP3*	0.886	0.676	0.037	0.818	8|0
53	Fatty acid binding protein 4, adipocyte	*FABP4*	0.886	0.640	0.162	0.679	8|7
54	Heat shock protein 90 kD β (Grp94), 1	*HSP90B1*	0.963	0.484	0.249	0.840	8|6
55	Uncoupling protein 2	*UCP2*	0.808	0.465	0.043	0.558	1|1
56	Uncoupling protein 3	*UCP3*	0.674	0.658	0.230	0.656	8|7
g	Transcription factors related to adipocyte differentiation						
	$P_{\text{ErminеJ}}$ (n_g=3)		0.088	1.000	0.937	1.000	
57	Adipocyte determination and differentiation factor 1	*ADD1*	0.505	0.484	0.655	0.558	8|8
58	CCAAT/ enhancer binding protein α	*CEBPA*	0.963	0.591	0.357	0.688	8|7
59	Peroxisome proliferator-activated receptor γ	*PPARG*	0.886	0.838	0.321	0.897	8|7
h	Regulatory factors of somatotropic axis						
	$P_{\text{ErminеJ}}$ (n_h=6)		0.077	0.319	0.789	1.000	
60	Growth hormone receptor	*GHR*	0.886	0.426	0.302	0.558	8|4
61	Insulin-like grouth factor l	*IGF1*	0.674	0.465	0.204	0.933	8|6
62	Insulin-like growth factor 2	*IGF2*	0.674	0.235	0.067	0.656	2|3
63	Insulin-like growth factor binding protein 2	*IGFBP2*	0.674	0.465	0.169	0.558	0|2
64	Insulin-like growth factor binding protein 3	*IGFBP3*	0.958	0.184	0.043	0.558	2|2
65	Insulin-like growth factor binding protein 5	*IGFBP5*	0.886	0.551	0.202	0.558	1|7

(*To be continued on the next page*)

(*Continued*)

ID	Gene name/ gene-group description	Gene symbol	P_1	P_2	P_3	P_4	Cluster ID
i	Myogenic determination factors (MDFs)						
	P_{ErmineJ} (n_i=6)		0.002	0.323	0.893	1.000	
66	Four and a half LIM domains 1	*FHL1C*	0.845	0.447	0.577	0.558	1|2
67	Myocyte enhancer factor 2B	*MEF2B*	0.149	0.465	0.622	0.558	3|8
68	Myocyte enhancer factor 2C	*MEF2C*	0.997	0.326	0.061	0.679	1|2
69	Myogenin	*MYOG*	0.886	0.235	0.302	0.558	8|8
70	Transforming growth factor β2	*TGFB2*	0.909	0.591	0.089	0.558	8|7
71	Transforming growth factor β3	*TGFB3*	0.886	0.484	0.160	0.897	8|6
j	Enzymes, regulatory proteins and binding proteins related to skeletal muscle fiber development and growth						
	P_{ErmineJ} (n_j=16)		0.976	1.000	0.779	1.000	
72	Actin α1, skeletal muscle	*ACTA1*	0.963	0.447	0.245	0.796	1|2
73	Actin related protein 2/3 complex, subunit 3, 21 kD	*ARPC3*	0.886	0.754	0.355	0.558	6|8
74	Actin related protein 2/3 complex, subunit 5, 16 kD	*ARPC5*	0.958	0.426	0.374	0.601	1|2
75	Ferritin, heavy polypeptide 1	*FTH1*	0.886	0.603	0.325	0.796	2|0
76	Histone deacetylase 5	*HDAC5*	0.886	0.515	0.606	0.656	8|2
77	Gelsolin	*LOC396874*	0.963	0.492	0.144	0.558	2|0
78	Myoglobin	*MB*	0.886	0.235	0.036	0.567	1|2
79	Myotrophin	*MTPN*	0.963	0.838	0.489	0.796	6|3
80	Myosin heavy chain 2B	*MYH2B*	0.963	0.792	0.037	0.558	1|8
81	Myosin heavy polypeptide 7, cardiac muscle, β	*MYH7*	0.886	0.465	0.026	0.558	1|2
82	Myosin light polypeptide 1	*MYL1*	0.963	0.465	0.012	0.568	1|5
83	Ryanodine receptor 1	*RYR1*	0.997	0.591	0.016	0.558	1|5
84	Sirtuin 2	*SIRT2*	0.909	0.676	0.225	0.796	0|2
85	Titin-cap (telethonin)	*TCAP*	0.963	0.363	0.012	0.558	1|2
86	Troponin I type 1	*TNNI1*	0.886	0.363	0.026	0.558	1|2
87	Titin	*TTN*	0.997	0.515	0.016	0.558	1|5
k	Adipocytokines and receiptors						
	P_{ErmineJ} (n_k=4)		0.134	0.464	0.830	1.000	
88	Adiponectin receptor 2	*ADIPOR2*	0.693	0.326	0.216	0.558	8|7
89	Leptin	*OB*	0.886	0.447	0.043	0.558	8|8
90	Resistin	*RETN*	0.963	0.754	0.601	0.558	6|8
91	Tumor necrosis factor receptor superfamily, member 1A	*TNFRSF1A*	0.505	0.249	0.204	0.558	2|1
l	Others						
	P_{ErmineJ} (n_l=4)		1.000	0.994	0.747	1.000	
92	Connective tissue growth factor	*CTGF*	0.954	0.465	0.202	0.829	8|4
93	Cytochrome b5 type A (microsomal)	*CYB5A*	0.886	0.603	0.653	0.601	7|0
94	Cytochrome P450, family 2, subfamily E, polypeptide 1	*CYP2E1*	0.886	0.551	0.143	0.836	5|7
95	Translationally controlled tumor protein	*TCTP*	0.886	0.591	0.080	0.601	2|3

P_1, P_2, P_3 and P_4 are FDR adjusted permutation P values from the tests of breed effect across time, time effect across breeds, time effect in Landrace and time effect in Taihu pigs, respectively. P_{ErmineJ} is the Benjamini-Hochberg FDR-corrected P value based on GCT analysis, and "n" denotes the gene number for each gene-group. Expression pattern ID denotes the corresponding number of the specific STEM profile (Landrace|Taihu pigs) (Figure 4). Filtered genes are marked with a backslash (\).

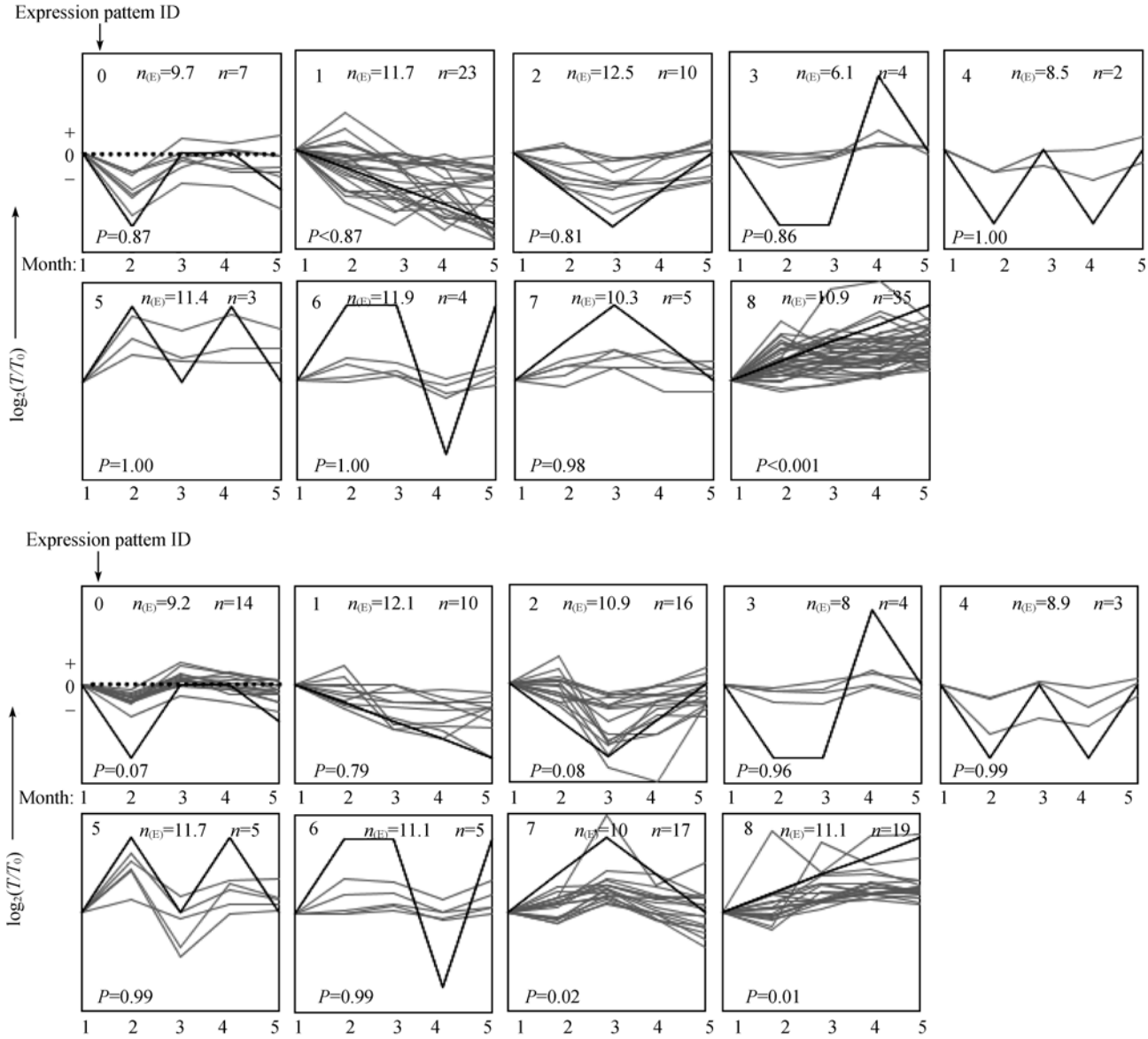

Figure 4 STEM clustering profiles for Landrace (a) and Taihu (b) pigs. The dashed line indicates no change in expression among different stages. The number in the top left corner of each square is the expression pattern ID. The black, bold lines in the squares are the trendlines of the expression patterns, and the gray lines represent the variational expression of genes from 1 to 5 months. *P* value is the corrected *P* value obtained from MHT.

2.5 Comparison of QRT-PCR and microarray data

QRT-PCR, a more sensitive and specific measure of gene expression, was performed on 5 selected genes to confirm differential expression as indicated by microarray. The average Pearson correlation coefficient between microarray and QRT-PCR expression data over all growth stages within each pig breed was 0.874± 0.071 (Table 3).

3 Discussion

Our results indicated that adipocyte volume and IMF content of the two pig breeds first decreased to a lowest value at 2-month but then gradually increased. These results can be explained by the idea that the growth and development of adipocytes during 2—5 months is the result of both increasing cell size (proliferation) and cell number (hypertrophy), but during 1—2 months only proliferation is predominant[21]. In addition, Taihu pigs had a higher adipocyte volume and IMF content than Landrace pigs at the same growth stage, which corresponds to their distinct breeding characteristics[5,22].

It is important to note that the ANOVA based on an empirical Bayes test generates five kinds of *P* values: a

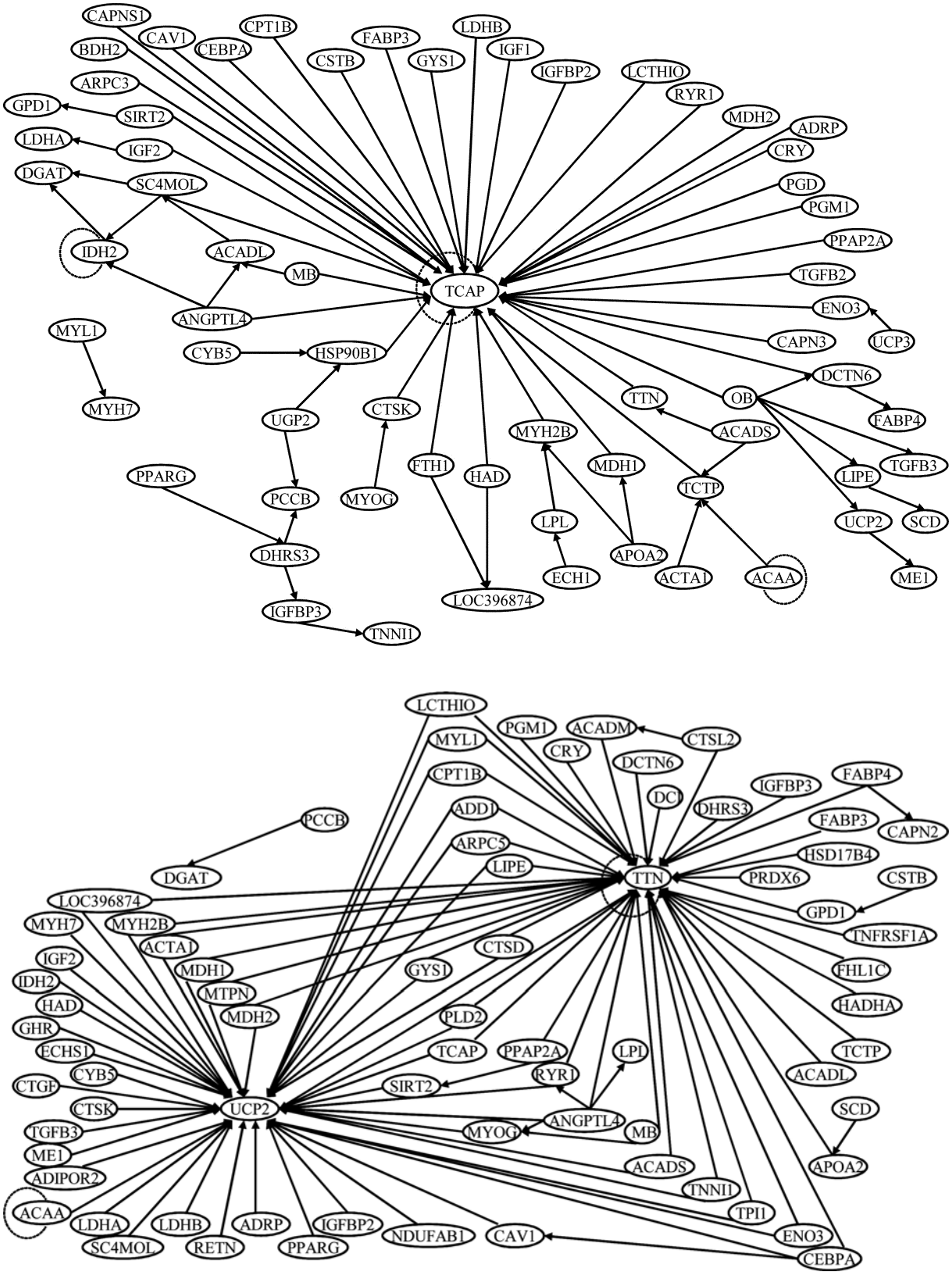

Figure 5 Regulatory networks of genes associated with meat quality and carcass traits in Landrace (a) and Taihu (b) pigs. Each straight arrow, from tail to head, indicates a parent-node-to-child-node relationship and the circular arrows represent self-regulation.

Table 3 Correlation test of measured gene expression changes between microarray and QRT-PCR

Gene symbol	Breed	Pearson correlation coefficient	*P* value
IGF-II	Landrace	0.975	0.005
	Taihu	0.875	0.052
IGFBP3	Landrace	0.986	0.002
	Taihu	0.894	0.041
SCD	Landrace	0.781	0.119
	Taihu	0.768	0.130
ME1	Landrace	0.851	0.068
	Taihu	0.874	0.053
UCP3	Landrace	0.838	0.076
	Taihu	0.902	0.036

tabulated *P* value based on assuming an *F* distribution, an FDR adjusted tabulated *P* value, a nominal permutation *P* value, an FDR adjusted permutation *P* value, and a family-wise error rate (FWER) one-step adjusted *P* value[23]. Both Allison et al.[24], and Yang and Churchill[25] suggested that the FDR adjusted permutation *P* value should be adopted first; however an FDR adjusted permutation *P* value is excessively restrictive, and biologists should consider other *P* values based on the actual demands of their research. Using FDR adjusted permutation *P* values, we found that no gene was significantly altered in Taihu pigs among five growth stages ($P>0.05$). However, there were 2 genes that showed differential expression at $P<0.01$ and 5 genes at $P<0.05$ in Taihu pigs over all growth stages using a nominal permutation *P* value. We still exclusively used an FDR adjusted permutation *P* value to highlight interesting genes, because the ranking of genes based on their variational degrees was almost uniform among the five kinds of *P* values, and our goal in this study was to find potential key genes with dramatic variation. Also, the GCT analysis provides additional statistical support to the findings and can improve the sensitivity of the analysis by statistically evaluating genes in biologically meaningful groups instead of individually. A typical goal is to determine whether particular biological pathways are "doing something interesting" in the data. A low P_{ErmineJ} value for a gene-group does not imply that all genes in the group show significantly altered expression. The rationale for including genes displaying subtle alterations in expression levels is based on the concept that such genes may be highly relevant to the biological functions of the different experimental conditions when viewed in the larger context of interacting genes. Genes not selected as differentially expressed might still have a positive impact on the gene-group; thus, this approach preserves information contained in the P_{ErmineJ}.

The results of ANOVA indicated that 25 genes in Landrace pigs and no genes in Taihu pigs showed differential expression at $P<0.05$ during the period from 1 to 5 months. These findings suggest that the metabolism in backfat is more active in Landrace pigs than in Taihu pigs during this important phase of pig development, which is consistent with the fact that the ability for fat deposition is lower in Landrace pigs than in Taihu pigs. The results also indicate that these genes may be subject to special regulation and exhibit dramatic expression changes according to their particular biological functions at different developmental stages. A multitude of studies have proven most of these differential expression genes to have an important influence on porcine meat quality and carcass composition, such as *FABP3*, *LPL*, *ME1*, *SCD* and *UCP2*. *FABP3*, a member of the FABP family, plays an essential role in long-chain fatty acid uptake and metabolic homeostasis[26]. Arnyasi et al.[27] reported that *FABP3* polymorphisms might explain as much as 30%—35% of the variation in IMF in their pig cross-population. Li et al.[28] found that *FABP3* mRNA was induced during adipogenic differentiation of stromal-vascular cells derived from porcine adipose tissue and skeletal muscle. *LPL* is a rate-limiting enzyme that hydrolyzes circulating triglyceride-rich lipoproteins, such as very low density lipoproteins and chylomicrons[29], and was studied as a candidate gene for having a major effect on porcine BFT. *ME1* is a part of the tricarboxylate shuttle that provides NADPH and acetyl-CoA, which are required in fatty acid biosynthesis[30]. Vidal et al.[31] demonstrated that *ME1* genotypes were significantly associated with BFT in Landrace pigs. *SCD* is the major gene target of leptin—a central mediator of energy homeostasis[32]. Doran et al.[33] found that a reduced protein diet induced *SCD* protein expression in pig muscle but not in subcutaneous adipose tissue, and as a result they thought that the *SCD* isoform spectra in pig subcutaneous adipose tissue and muscle might be different. *UCP2* expression in adipose and muscle is postulated to be involved in the regulation of energy expenditure and nutrient partitioning, particularly that of fats[34]. Li et al.[35] found that the genotype, compounding of seven deletion sites, three in *UCP2* and four in

UCP3, in 15 pig breeds had significant effects on porcine body weight.

However, there is little information available in the literature about the relationship between the remaining 7 genes (*ANGPTL4*, *DHRS3*, *ECHS1*, *ENO3*, *PCCB*, *PGM1* and *SC4MOL*) and economically relevant porcine traits. Further work may be needed to definitely determine the effects of the above genes on the phenotypes of porcine adipose and skeletal muscle tissue, because the functions of these genes are closely associated with fatty acid metabolism and cell growth regulation. It is noteworthy that the main function of *ANGPTL4*—a member of the angiopoietin-like family of proteins, is to regulate triglyceride metabolism by inhibiting the activity of *LPL*. Given the central role of *LPL* in energy metabolism, the multifunctional *ANGPTL4* holds great potential for applications in biomedical research and animal agriculture[36]. Feng et al.[37] reported the coding region (1239 bp) sequence for porcine *ANGPTL4* gene and mapped it to chromosome 2q21→q24 region by radiation hybrid mapping. Strikingly, many other microsatellite markers, quantitative trait loci (QTL) and functional genes associated with porcine economic traits, such as IMF content, backfat thickness and lean meat percentage in the carcass, were also located in close proximity on the chromosome. Up to now, related research has mainly focused on novel therapeutic targets for human metabolic syndrome; relatively little knowledge relevant to animal (pigs) production is available. We tentatively suggest that, as a possible candidate gene affecting porcine fat traits, *ANGPTL4* is worth studying intensively.

On the basis of the strict criteria of GCT, expression level of gene-group "a" was significantly altered between two pig breeds during the period from 1 to 5 months ($P_{\text{ErminеJ}}$<0.01) (Table 2). This representative gene-group consisted of 23 genes encoding enzymes and regulatory proteins related to lipid and steroid metabolism, which accounted for 24.21% of the total of 95 genes. These findings suggest that the distinct differences in fat deposition ability between Landrace and Taihu pigs may closely correlate with the expression changes of these genes.

To date, most papers presenting short time-series datasets use one of the standard clustering methods (such as hierarchical clustering[38], *k*-means clustering[39] and self-organizing maps[40]) to analyze their data. These methods, however, both assume that data at each time point is collected independent of each other, ignoring the sequential nature of time series data. More recently, a number of clustering algorithms specifically designed for time-series expression data were suggested. These algorithms mainly include clustering based on the dynamics of the expression patterns[41], clustering using the continuous representation of the profile[42] and clustering using a hidden Markov model (HMM)[43]. While these algorithms work well for relatively long time-series datasets (10 time points or more), they will overfit the data when the number of time points is small, so many patterns can be expected to appear at random. To our knowledge, only STEM is designed specifically for the analysis of short time-series data (3－8 time points), which can distinguish between real and random patterns[44].

The results of STEM clustering indicated that the predominant expression patterns in Landrace pigs were 1 and 8, which included 23 and 35 genes (P<0.01), respectively, while the representative expression patterns in Taihu pigs were 7 and 8, which only included 17 and 19 genes (P<0.05), respectively (Figure 4). Thus, it can be known that expression patterns of genes related to meat quality and carcass traits in backfat across five growth stages were more dispersed in Taihu pigs than in Landrace pigs. This finding suggests that the intracellular regulatory relationships of micro-effect polygenes, which influence physiological and biochemical aspects of adipose deposition, are more complex in Taihu pigs than in Landrace pigs, and this may be due to the fact that the fat deposition ability of Taihu pigs is higher than that in Landrace pigs. Notably, expression pattern 8 in Landrace pigs was the most predominant temporal pattern of the total of eight patterns in two pig breeds, which included 35 genes and accounted for 37.63% of the total of 93 genes. This pattern represented genes that strongly up-regulated from 1 to 5 months. By classifying genes based on the genes' biological functions, we found that most genes with expression pattern 8 in Landrace pigs, such as *ECH1*, *OB*, *PCCB*, *ADIPOR2*, *DCI* and *DHRS3*, were linked to the positive regulation of fatty acid β-oxidation. This finding indicates that the transcript abundances of genes that accelerate energy consumption rise, which may result in Landrace pigs having a lower BFT and IMF content than Taihu pigs.

Inferring GRNs, that is, how all the functional molecules of these networks exist, interact and react spatio-

temporally, is a major focus of interest in modern boiology. In recent years, a number of methods have been proposed for modelling GRNs including: Boolean networks[45], Linear models[46], Graphical Gaussian models (GGMs)[47], differential equations[48], DBNs[18], etc. In particular, researchers have paid great attention to DBNs, which model causal relationships between variables based on probabilistic measure. When we have time-series datasets, the use of DBNs is a promising alternative, since DBNs can treat time delay information and construct cyclic networks.

By comparing the inferred interactions between genes with the corresponding pathways through KEGG on-line database, we found that many of the inferred gene relations are known to be involved in the pathways, along with the experimental validation. For instance, *OB* was a primary leading parent node of a GRN in Landrace pigs, which directly regulated *LIPE* and *UCP2*. Leptin, the product of the *OB* gene, plays a major role in appetite suppression and regulation of energy expenditure, which is the best known hormone markers for obesity[49]. O'Rourke et al.[50] demonstrated that Leptin significantly increased *LIPE* activity in human J774.2 macrophages. Rance et al.[51] found an association between human leptin and A55V of the *UCP2* gene (−866G>A and exon-8 ins/del) (P<0.01), so they suggested that the A55V polymorphism directly affected the levels of leptin. There were great discrepancies between the GRNs of the two pig breeds, an observation which hypothetically reveals the dissimilar molecular basis for adipose metabolism in lean Landrace versus fatty Taihu pigs. For example, the reconstructed sub-networks for Landrace and Taihu pigs showed that *LPL* was directly regulated by *ECH1* and *ANGPTL4*, respectively. The former interaction (*ECH1*→*LPL*) has not been verified by the experiments and thus can probably be categorized as a biological hypothesis requiring further experimental validation. The latter interaction (*ANGPTL4*→*LPL*) agrees with the experimental findings of *ANGPTL4* converting *LPL* to inactive monomers and modulating lipase activity in adipose tissue by Sukonina et al.[52].

It should especially be mentioned that any methodology to reconstruct GRNs should bear rich statistics and probability semantics because of the stochastics of gene expression events, the inherent limitation of the algorithm and the incoming randomness during the processes of gene selection and data sampling. As a tentative exploration, however, GRNs can help us to understand the likely regulatory relationships of genes at the system level and identify the potentially key genes for further research. In addition, 5 genes selected according to microarray analysis showed corresponding values by QRT-PCR with high positive correlation, which indicated that our microarray results reliably reveal the differences in gene expression profiles in backfat[53].

The present study provides a rich, new information resource that increases our understanding of the molecular mechanisms underlying porcine fat deposition. It is also proved that the knowledge-based, self-designed, pathway-focused microarray merges the benefits of hypothesis-driven and discovery-based research, allowing researchers to better characterize the biological system at hand and answer more specific questions in a systematic fashion.

1 Fiedler I, Nürnberg K, Hardge T, et al. Phenotypic variations of muscle fibre and intramuscular fat traits in *longissimus* muscle of F_2 population Duroc×Berlin Miniature Pig and relationships to meat quality. Meat Sci, 2003, 63: 131－139

2 Plastow G S, Carrión D, Gil M, et al. Quality pork genes and meat production. Meat Sci, 2005, 70: 409－421

3 Suzuki K, Irie M, Kadowaki H, et al. Genetic parameter estimates of meat quality traits in Duroc pigs selected for average daily gain, *longissimus* muscle area, backfat thickness, and intramuscular fat content. J Anim Sci, 2005, 83: 2058－2065

4 Ailhaud G. Adipose tissue as a secretory organ: From adipogenesis to the metabolic syndrome. C R Biol, 2006, 329: 570－577

5 Editorial Committee of "Pig Breeds in China". Pig Breeds in China (in Chinese). Shanghai: Scientific & Technical Publishing House, 1986. 155－160

6 Khatri P, Bhavsar P, Bawa G, et al. Onto-Tools: An ensemble of web-accessible, ontology-based tools for the functional design and interpretation of high-throughput gene expression experiments. Nucleic Acids Res, 2004, 32(Web Server issue): W449－W456

7 Doms A, Schroeder M. GoPubMed: Exploring PubMed with the Gene Ontology. Nucleic Acids Res, 2005, 33(Web Server issue): W783－W786

8 Yang Y H, Speed T. Design issues for cDNA microarray experiments. Nat Rev Genet, 2002, 3: 579－588

9 Yang Y H, Dudoit S, Luu P, et al. Normalization for cDNA microarray data: A robust composite method addressing single and multiple slide systematic variation. Nucleic Acids Res, 2002, 30(4): e15－e24

10 Xia X, McClelland M, Wang Y. WebArray: An online platform for

microarray data analysis. BMC Bioinformatics, 2005, 6: 306－311
11 Smyth G K, Michaud J, Scott H S. Use of within-array replicate spots for assessing differential expression in microarray experiments. Bioinformatics, 2005, 21: 2067－2075
12 Troyanskaya O, Cantor M, Sherlock G, et al. Missing value estimation methods for DNA microarrays. Bioinformatics, 2001, 17: 520－525
13 Kerr M K, Martin M, Churchill G A. Analysis of variance for gene expression microarray data. J Comput Biol, 2000, 7: 819－837
14 Cui X, Hwang J T, Qiu J, et al. Improved statistical tests for differential gene expression by shrinking variance components estimates. Biostatistics, 2005, 6: 59－75
15 Lee H K, Braynen W, Keshav K, et al. ErmineJ: Tool for functional analysis of gene expression data sets. BMC Bioinformatics, 2005, 6: 269－276
16 Ernst J, Bar-Joseph Z. STEM: A tool for the analysis of short time series gene expression data. BMC Bioinformatics, 2006, 7: 191－121
17 Wu C C, Huang H C, Juan H F, et al. GeneNetwork: An interactive tool for reconstruction of genetic networks using microarray data. Bioinformatics, 2004, 20: 3691－3693
18 Dojer N, Gambin A, Mizera A, et al. Applying dynamic Bayesian networks to perturbed gene expression data. BMC Bioinformatics, 2006, 7: 249－259
19 Erkens T, Van Poucke M, Vandesompele J, et al. Development of a new set of reference genes for normalization of real-time RT-PCR data of porcine backfat and *longissimus dorsi* muscle, and evaluation with PPARGC1A. BMC Biotechnol, 2006, 6: 41－48
20 Vandesompele J, De Preter K, Pattyn F, et al. Accurate normalization of real-time quantitative RT-PCR data by geometric averaging of multiple internal control genes. Genome Biol, 2002, 3: 34－45
21 Anderson D B, Kauffman R G. Celluar and enzymatic changes in porcine adipose tissue during growth. J Lipid Res, 1973, 14: 160－168
22 Kolstad K. Fat deposition and distribution measured by computer tomography in three genetic groups of pigs. Livest Prod Sci, 2001, 67: 281－292
23 Datta S, Datta S. Empirical Bayes screening of many *P* values with applications to microarray studies. Bioinformatics, 2005, 21: 1987－1994
24 Allison D B, Cui X, Page G P, et al. Microarray data analysis: From disarray to consolidation and consensus. Nat Rev Genet, 2006, 7: 55－65
25 Yang H, Churchill G. Estimating *P* values in small microarray experiments. Bioinformatics, 2007, 23: 38－43
26 Chmurzyńska A. The multigene family of fatty acid-binding proteins (FABPs): Function, structure and polymorphism. J Appl Genet, 2006, 47: 39－48
27 Arnyasi M, Grindflek E, Jávor A, et al. Investigation of two candidate genes for meat quality traits in a quantitative trait locus region on SSC6: The porcine short heterodimer partner and heart fatty acid binding protein genes. J Anim Breed Genet, 2006,123: 198－203
28 Li B, Zerby H N, Lee K. Heart fatty acid binding protein is up-regulated during porcine adipocyte development. J Anim Sci, 2007, 85: 1651－1659
29 Du J K, Huang Q Y. Research progress of lipoprotein lipase gene. Yi Chuan (in Chinese), 2007, 29: 8－16
30 Hsu W C, Hung H C, Tong L, et al. Dual functional roles of ATP in the human mitochondrial malic enzyme. Biochemistry, 2004, 43: 7382－7390
31 Vidal O, Varona L, Oliver M A, et al. Malic enzyme 1 genotype is associated with backfat thickness and meat quality traits in pigs. Anim Genet, 2006, 37: 28－32
32 Sampath H, Miyazaki M, Dobrzyn A, et al. Stearoyl-CoA desaturase-1 mediates the pro-lipogenic effects of dietary saturated fat. J Biol Chem, 2007, 282: 2483－2493
33 Doran O, Moule S K, Teye G A, et al. A reduced protein diet induces stearoyl-CoA desaturase protein expression in pig muscle but not in subcutaneous adipose tissue: Relationship with intramuscular lipid formation. Br J Nutr, 2006, 95: 609－617
34 Brand M D, Esteves T C. Physiological functions of the mitochondrial uncoupling proteins UCP2 and UCP3. Cell Metab, 2005, 2: 85－ 93
35 Li Y, Li H, Zhao X, et al. UCP2 and 3 deletion screening and distribution in 15 pig breeds. Biochem Genet, 2007, 45: 103－111
36 Li C. Genetics and regulation of angiopoietin-like proteins 3 and 4. Curr Opin Lipidol, 2006, 17: 152－156
37 Feng S Q, Chen X D, Xia T, et al. Cloning, chromosome mapping and expression characteristics of porcine *ANGPTL3* and *-4*. Cytogenet Genome Res, 2006, 114: 44－49
38 Eisen M B, Spellman P T, Brown P O, et al. Cluster analysis and display of genome-wide expression patterns. Proc Natl Acad Sci USA, 1998, 95: 14863－14868
39 Tavazoie S, Hughes J D, Campbell M J, et al. Systematic determination of genetic network architecture. Nat Genet, 1999, 22: 281－285
40 Tamayo P, Slonim D, Mesirov J, et al. Interpreting patterns of gene expression with self organizing maps: methods and applications to hematopoietic differentiation. Proc Natl Acad Sci USA, 1999, 96: 2907－2912
41 Ramoni M F, Sebastiani P, Kohane I S. Cluster analysis of gene expression dynamics. Proc Natl Acad Sci USA, 2002, 99: 9121－9126
42 Bar-Joseph Z, Gerber G K, Gifford D K, et al. Continuous representations of time-series gene expression data. J Comput Biol, 2003, 10: 341－356
43 Schliep A, Schönhuth A, Steinhoff C. Using hidden Markov models to analyze gene expression time course data. Bioinformatics, 2003, 19 (Suppl 1): 255－263
44 Ernst J, Nau G J, Bar-Joseph Z. Clustering short time series gene ex-

pression data. Bioinformatics, 2005, 21(Suppl 1): 159－168
45 Raeymaekers L. Dynamics of Boolean networks controlled by biologically meaningful functions. J Theor Biol, 2002, 218: 331－341
46 D'haeseleer P, Wen X, Fuhrman S, et al. Linear modeling of mRNA expression levels during CNS development and injury. Pac Symp Biocomput, 1999, 4: 41－52
47 Werhli A V, Grzegorczyk M, Husmeier D. Comparative evaluation of reverse engineering gene regulatory networks with relevance networks, Graphical Gaussian models and Bayesian networks. Bioinformatics, 2006, 22: 2523－2531
48 de Hoon M J, Imoto S, Kobayashi K, et al. Inferring gene regulatory networks from time-ordered gene expression data of *Bacillus subtilis* using differential equations. Pac Symp Biocomput, 2003, 8: 17－28
49 Zhang F, Chen Y, Heiman M, et al. Leptin: Structure, function and biology. Vitam Horm, 2005, 71: 345－372
50 O'Rourke L, Yeaman S J, Shepherd P R. Insulin and leptin acutely regulate cholesterol ester metabolism in macrophages by novel signaling pathways. Diabetes, 2001, 50: 955－961
51 Rance K A, Johnstone A M, Murison S, et al. Plasma leptin levels are related to body composition, sex, insulin levels and the A55V polymorphism of the *UCP2* gene. Int J Obes, 2007, 31: 1311－1318
52 Sukonina V, Lookene A, Olivecrona T, et al. Angiopoietin-like protein 4 converts lipoprotein lipase to inactive monomers and modulates lipase activity in adipose tissue. Proc Natl Acad Sci USA, 2006, 103: 17450－17455
53 Qin L X, Beyer R P, Hudson F N, et al. Evaluation of methods for oligonucleotide array data via quantitative real-time PCR. BMC Bioinformatics, 2006, 7: 23－34